Plasma reforming of biomass gasification tars using mixed naphthalene and toluene as model compounds

Danhua Mei[1], Yaolin Wang[1], Shiyun Liu[1], Martin Alliati[1], Haiping Yang[2], Xin Tu[1*]

[1]Department of Electrical Engineering and Electronics, University of Liverpool, Liverpool L69 3GJ, United Kingdom

[2]State Key Laboratory of Coal Combustion, School of Energy and Power Engineering, Huazhong University of Science and Technology, 430074 Wuhan, China

*Corresponding author (Dr. X. Tu)

Email: xin.tu@liverpool.ac.uk

Abstract

Non-equilibrium plasma technology provides an unconventional but promising solution for the cleaning of tar contaminated bio-syngas in biomass gasification. This work is focused on the reforming of mixed naphthalene ($C_{10}H_8$) and toluene (C_7H_8) as a typical single ring and double ring tar model components using a gliding arc discharge (GAD) reactor. The influence of naphthalene content, steam/carbon ratio and plasma power on the destruction of $C_{10}H_8$ and C_7H_8 was evaluated to understand their effects on the tar conversion, gas yield, and the energy consumption. Adding H_2O to the plasma process forms OH radicals, creating additional reaction routes for the step-wised oxidation of naphthalene, toluene and their fragments towards the production of CO, CO_2, and water. The highest decomposition of naphthalene and toluene (~80% overall) was obtained when the optimum steam/carbon molar ratio changed between 1.0 and 1.5, which was dependent on the balance between two opposite effects due to the presence of steam: positive effect of OH radicals and negative effect of electron attachment on water molecules. The highest energy efficiency (53.6 g/kWh) was obtained for the destruction of mixed tar compounds, which is by far the highest in previously reported works. CO, H_2 and C_2H_2 were the major gases with the highest CO yield of 38.6% and H_2 yield of 39.1%. Emission spectroscopic diagnostics was employed to understand the contribution of chemically active species to the GAD reaction. Possible reaction pathways in the plasma reduction of mixed naphthalene and toluene were proposed based on the plasma spectroscopic diagnostics coupled with a comprehensive analysis of major gas products and condensable by-products.

Keywords: Non-thermal plasma; Gliding arc; Naphthalene; Toluene; Tar; Biomass gasification

1. Introduction

Biomass is an important renewable and sustainable energy source to tackle global warming and CO_2 emission. Biomass gasification is a major thermochemical process to produce bio-syngas (CO and H_2), which can be further used for generating heat and electricity or for the synthesis of higher value chemicals. The contamination of bio-syngas with tars has been highlighted as a key challenge in biomass gasification processes. Tar is a mixture of complex condensable hydrocarbons, containing aromatics and multiple-ring polycyclic aromatics [1, 2]. Typically, the content of tars in raw bio-syngas varies from 1 to 100 g/Nm^3 and is dependent on the processing conditions and the type of gasifiers, while the acceptable level of tars for gas turbines and combustion engines are 5 and 100 mg/Nm^3, respectively [3]. The presence of tars with a high content in the produced bio-syngas can cause critical fouling, blocking and corrosion problems, limiting the use of bio-syngas for more extensive energy applications particularly in the synthesis of chemical feedstocks. Therefore, cost-effective removal of tars from produced raw bio-syngas has been is crucial for the successful implementation of biomass gasification technology in the bioenergy industry [3, 4].

Different approaches are presently being investigated for tar removal, including physical removal, thermal cracking and catalytic cracking [4-9]. Physical removal processes use filters, cyclones, electrostatic precipitators (ESPs) or scrubbers to separate tars after condensation. The energy content of the tars is usually wasted in this process, reducing the overall efficiency of this process, while the post-disposal of collected tars is one of the disadvantages of this process. Also, the wet cleaning process generates large amounts of contaminated water, requiring downstream further treatment or recycling. Although physical removal process offers a reliable and effective solution for tar elimination, it is more energy consuming and more

expensive to operate compared to other processes [4]. Thermal or catalytic cracking can convert tars into light gases. However, high temperatures (>1000 ^{o}C) are usually required for thermal cracking to achieve sufficient tar conversion in realistic residence time, incurring high energy cost and producing agglomerated soot particles [8]. Catalytic tar cracking at high temperatures (750-900 ^{o}C) has been regarded as a possible solution for the generation of clean bio-syngas [4, 10, 11]. However, catalyst deactivation and long-term stability due to coke deposition on the catalyst surfaces remain a major barrier to use this process on an industrial scale. Developing cost-effective, highly active and stable catalysts is the key and a long-term target for thermal catalytic reforming of tars from gasification.

Non-thermal plasma (NTP) has been recognized as an emerging and alternative solution to conventional approaches for tar reduction in biomass gasification at low temperatures and ambient pressure [12-14]. NTP generates energetic electrons together with reactive species including excited species, which can break benzene rings or chemical bonds of tars and enable thermodynamically unfavorable reactions to proceed at ambient conditions [15, 16]. NTP processes can be started up and switched off instantly due to the fast reaction, offering great potential to be integrated with sustainable energy (e.g., wind and solar power) for chemical energy storage.

Although great efforts have been expended on the removal of diluted low concentration volatile organic compounds (VOCs) and the conversion of small carbon molecules (e.g., CH_4, CO_2, and methanol) to fuels and chemicals using NTP[17-24], far less has been done on the plasma reforming of tars for both bio-syngas cleaning and energy recovery [25-30]. The reduction or conversion of large carbonic molecules (e.g., benzene, toluene, and naphthalene) in the form of tar surrogates remains a challenge when using non-thermal plasmas due to potential carbon

deposition and polymerization of tar compounds in the reaction especially when using glow discharges and dielectric barrier discharges as the concentration of tars in these processes is significantly higher (1-3 orders of magnitude higher) in comparison to the concentration of these large carbon molecules in the form of either VOCs or polycyclic aromatic hydrocarbons (PAHs) from combustion.

Up until now, limited works have been done to have a comprehensive understanding of the plasma decomposition of typical tar model components given that plasma tar reforming is still a very complex process involving numerous active species and a great number of chemical reactions. Also, most of the previous studies focused on the conversion of a single tar model compound (mainly toluene and benzene) with a single benzene ring using plasma reforming [31, 32]. For instance, Zhu et al. investigated the influence of toluene feed concentration and nitrogen flow rate on the conversion of toluene in the absence of steam in a GAD reactor. C_2H_2 and H_2 were found as the valuable primary products [32]. Recently, Wnukowski et al. compared the effects of gas composition on benzene conversion in a microwave plasma and found that adding CO_2, H_2 N_2, and H_2O was beneficial to the plasma processing of benzene, while the addition of CH_4 decreased the benzene conversion [31, 33].

However, tar, as a mixture of complex condense liquid hydrocarbons, contains a great number of single to multiple ring aromatics and complex PAHs [1]. Therefore, understanding the plasma reforming of mixed tar model compounds (e.g., mixed typical single ring and double ring tar compounds), especially a comprehensive analysis of tar destruction, gas yield, by-product production and process efficiency, is of critical importance to gain new insights into the plausible reaction mechanism driven by new reactive species formed in the plasma process and to generate new and valuable knowledge to make the plasma tar reforming process more

attractive and competitive. Unfortunately, very limited works on the use of NTP processes for the reforming of mixed tar surrogates (e.g., mixed naphthalene and toluene) has been reported. Additionally, a comprehensive understanding of the plasma chemistry and reaction mechanism in the plasma interactions with both single ring and double ring large carbon molecules is still missing.

In this study, an atmospheric gliding arc discharge (GAD) reactor with knife-shaped electrodes was developed for the reforming of mixed tar compounds. GAD has been demonstrated to be very effective for the decomposition of carbon-based molecules including both small (e.g., CH_4 and CO_2) and large carbon molecules (e.g., toluene) compared to other types of NTP such as corona and DBD, due to significantly higher electron density generated in a GAD. Toluene and naphthalene represent typical tar compounds (single ring and double ring) from biomass gasification, diluted in a nitrogen flow [6]. Different process parameters (e.g., initial concentration of tar mixture, discharge power and steam/carbon molar ratio) have been evaluated to understand their effects on the plasma reforming of mixed tar compounds such as the destruction of naphthalene and toluene, the yield of major gases and the process efficiency. Plasma spectroscopic diagnostics was employed to reveal the production and the roles of these chemically active species in the reaction. In addition, the contributions of nitrogen excited species and oxidative species (from H_2O dissociation) to the conversion of tar mixture compounds have been investigated at different humidity levels. The plausible process mechanism in the plasma processing of naphthalene and toluene was proposed through plasma spectroscopic diagnosis combined with the analysis of major gas and liquid products.

2. Experimental

2.1 Experimental setup

Fig.1 presents the scheme of the reforming system including a lab-scale GAD reactor with two stainless steel knife-shaped electrodes (1.8 cm wide and 6 cm long). The minimum electrode gap was 2 mm for the initial arc formation. Nitrogen was acted as a dilution gas at a fixed flow rate of 3.5 L/min. The plasma reaction volume of the gliding arc reactor was around 3.5 ml and the residence time of the reactants in the arc zone was around 1 s. A mixed stream of naphthalene (purity >= 99%, Aldrich), toluene (purity >= 99%, Aldrich), deionized water and carrier gas were preheated to 300 ^{o}C in a tube furnace before injecting to the plasma reactor. The flow of naphthalene/toluene mixture and deionized water was controlled by two syringe pumps (KDS Legato 100), respectively. The content of naphthalene was quite low compared to toluene in the typical composition of biomass tar. Thus, the concentration of naphthalene was chosen much lower than that of toluene in this study. To understand the influence of steam on tar reduction, the ratio of steam/carbon can be adjusted between 0 and 2.5. The GAD reactor was powered by a neon high voltage transformer (max 10 kV peak-peak) and a fixed frequency (50 Hz). The electrical signals (arc current I and arc voltage U) were sampled by a Tektronix oscilloscope (MDO3024).

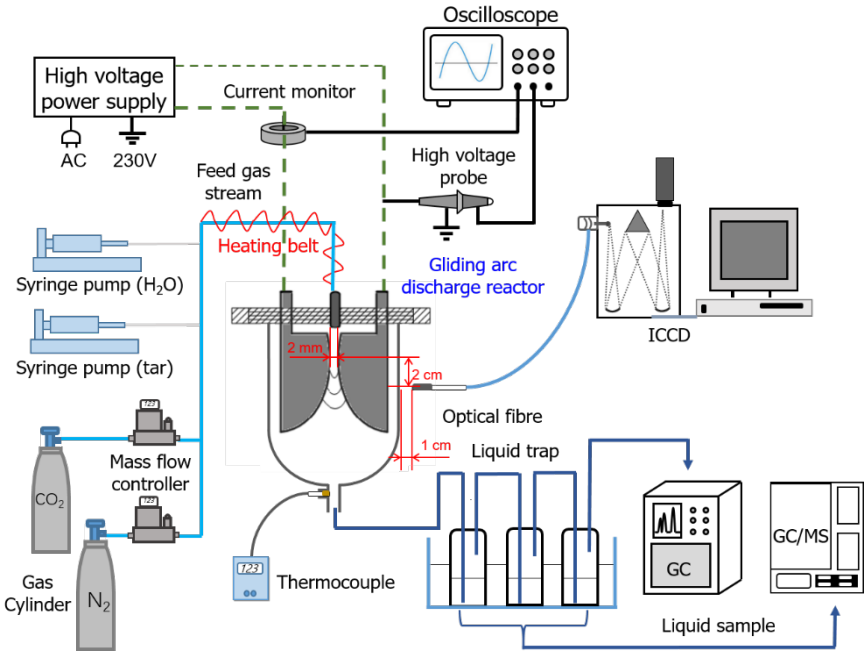

Fig. 1. Scheme of GAD plasma tar reforming system

2.2 Analysis of products

The products were measured after running the plasma reaction for about 20 mins when a steady state of the plasma reaction was reached. The gas products were collected using a sampling bag and measured by two-channel gas chromatography (Shimadzu GC-2014) equipped with a flame ionization detector (FID) and a thermal conductivity detector (TCD). Ar was used as a carrier gas with a flow rate of 50 ml/min. The first channel of the GC contained a Molecular Sieve 5A (60-80 mesh) column for the separation of H_2 and CO, while the second channel was equipped with a HayeSep N (60-80 mesh) column for the measurement of CO_2, CH_4 and C_2-C_4 hydrocarbons. The initial column temperature of the GC was 50 ^oC, holding for 3.5 mins. After that, the temperature increased to 160 ^oC at a heating rate of 60 ^oC/min, then kept for 30 mins. The GC was calibrated for each gaseous component with a wide range of concentrations using standard gas mixtures (Air Liquid). An ice-cold trap including three successive absorption bottles was used for collecting the condensable liquid chemicals. The first two bottles contain dichloromethane (DCM) to absorb condensable products, and the last bottle was kept empty to collect remaining entrained droplets. The total volume of DCM in the first two bottles was 100 ml. The condensed liquid products were detected by an Agilent GC - mass spectrometry (7820A/5975C) and analyzed using the standard library of the NIST (National Institute of Standards and Technology). Each analysis was repeated for three times when the NTP reaction reached a steady state in about 20 mins. Optical emission spectroscopic diagnostics of the GAD plasma was carried out by using a Princeton Instruments ICCD spectrometer (Model-320-PI) with a focal length of 320 mm. An optical fiber was connected to the spectrometer to record the emission spectra of the GAD under different experimental conditions. The optical fiber was placed at 2 cm downstream of the electrode throat on the plasma jet axis (Fig. 1). The gas temperature at the outlet of the GAD reactor was measured

using a thermocouple, as shown in Fig. 1. Typical time evolution of the gas temperature can be found in Fig. 2. After running the experiment for around 10 mins, the gas temperature at the outlet of the GAD reactor was almost constant (< 290 ^{o}C) at an input power of 59.4 W and reached up to 325 ^{o}C when further increasing the input power to 73 W.

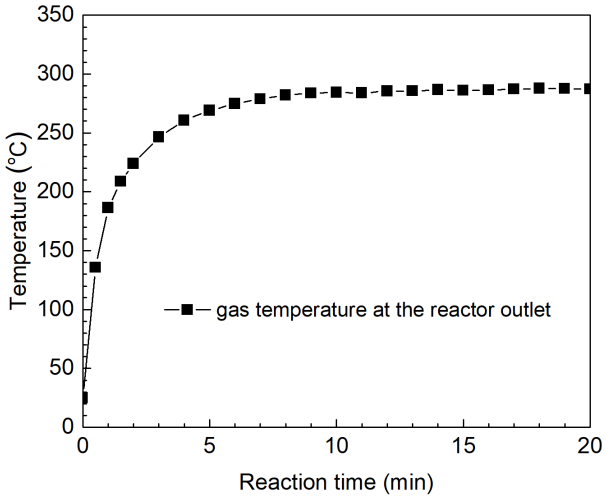

Fig. 2. The gas temperature at the outlet of the GAD reactor (C_7H_8 content: 17.3 g/Nm^3; $C_{10}H_8$ content: 1.0 g/Nm^3; discharge power: 59.4 W)

2.3 Definition of parameters

The plasma power P can be calculated through the integration of arc current (I) and arc voltage (U) .

$$P(\mathrm{W}) = \frac{1}{T}\int_{0}^{t=T} U(t)\times I(t)\,dt \tag{1}$$

Specific input energy (SIE), a key parameter to evaluate the effectiveness of plasma chemical processes, is defined as,

$$SEI\left(\mathrm{kWh/m^3}\right) = \frac{P(\mathrm{kW})}{\text{Total gas flow rate}\ \left(\mathrm{m^3/h}\right)} \tag{2}$$

The conversion of tar (toluene or naphthalene) X_{tar} can be defined as:

$$X_{\text{tar}}(\%) = \frac{C_o - C_i}{\mathrm{C_i}} \times 100 \quad (3)$$

where C_i and C_o are the concentration of tar (toluene or naphthalene) before and after the reaction, respectively.

The yield of gas products can be calculated as:

$$Y_{\mathrm{H_2}}(\%) = \frac{\mathrm{H_2\ produced\,(mol/s)}}{4\times(\mathrm{C_7H_8}+\mathrm{C_{10}H_8})\ \mathrm{input\ (mol/s)}+\mathrm{H_2O\ input\,(mol/s)}} \times 100 \quad (4)$$

$$Y_{\mathrm{CO_x}}(\%) = \frac{\mathrm{CO_x\ produced\ (mol/s)}}{7\times\mathrm{C_7H_8}+10\times\mathrm{C_{10}H_8}\ \mathrm{input\ (mol/s)}} \times 100 \quad (5)$$

$$Y_{\mathrm{C_xH_y}}(\%) = \frac{x\times\mathrm{C_xH_y\ produced\ (mol/s)}}{7\times\mathrm{C_7H_8}+10\times\mathrm{C_{10}H_8}\ \mathrm{input\ (mol/s)}} \times 100 \quad (6)$$

The carbon balance of the plasma reforming process was determined by

$$B_{\text{Carbon}}(\%) = \frac{(7\times\mathrm{C_7H_8}+10\times\mathrm{C_{10}H_8})_{\text{unconverted}}\,\mathrm{(mol/s)} + x\times\mathrm{C_xH_{y\,produced}\ (mol/s)} + \mathrm{CO_{x\,produced}\ (mol/s)}}{(7\times\mathrm{C_7H_8}+10\times\mathrm{C_{10}H_8})_{\text{input}}\ \mathrm{(mol/s)}} \times 100 \quad (7)$$

The energy efficiency for tar reforming is given by

$$E(\mathrm{g/kWh}) = \frac{\text{mass of converted tar (g/h)}}{\text{discharg power (kW)}} \quad (8)$$

3. Results and discussion

3.1 Influence of steam/carbon ratio

Understanding the effect of gas humidity on tar reforming is of great interest as the bio-syngas in biomass gasification typically contains large amounts of water (~15 vol. %). To assess the contribution of steam to the reduction of mixed tar compounds, the ratio of steam/carbon was varied between 0 and 3.0 to examine its effect on the conversions of naphthalene and toluene

223 at 3.5 L/min and 59.4 W. As plotted in Fig. 3 (a), the naphthalene conversion increased initially
224 when increasing the steam/carbon ratio, reached a maximum of 63.0% at the steam/carbon ratio
225 of 1.0. This value was significantly decreased when further increasing the molar ratio of S/C to
226 3.0. Similarly, the highest toluene conversion of 79.2% was obtained at an optimum
227 steam/carbon ratio of 1.5, while changing the ratio of steam/carbon from 1.5 to 3.0 only slightly
228 decreased the conversion of toluene. The formation of OH radicals when adding H_2O to the
229 GAD system could create new reaction pathways for the step-wised oxidation of $C_{10}H_8$, C_7H_8
230 and their fragments (R1 and R2), resulted in a boost of the destruction of tars in comparison to
231 the plasma process with no steam. In the GAD plasma, OH radicals are mainly generated
232 through water dissociation by electrons (R3 and R4) and excited nitrogen species (R5). The
233 destruction of naphthalene and toluene can also be proceeded via the reaction with H radicals
234 to form products such as styrene, xylene, and benzene.

235 $$C_{10}H_8 + OH \rightarrow \text{Intermediates} + H_2O \quad \text{(R1)}$$

236 $$C_7H_8 + OH \rightarrow \text{Intermediates} + H_2O \quad \text{(R2)}$$

237 $$H_2O + e \rightarrow H + OH + e \quad \text{(R3)}$$

238 $$H_2O + N_2^* \rightarrow H + OH + N_2 \quad \text{(R4)}$$

239 $$N_2 + e \rightarrow N_2^* + e \quad \text{(R5)}$$

240 where N_2* represents excited N_2 species, which can be either N_2 metastable states $N_2(A^3)$ or
241 $N_2(a')$.

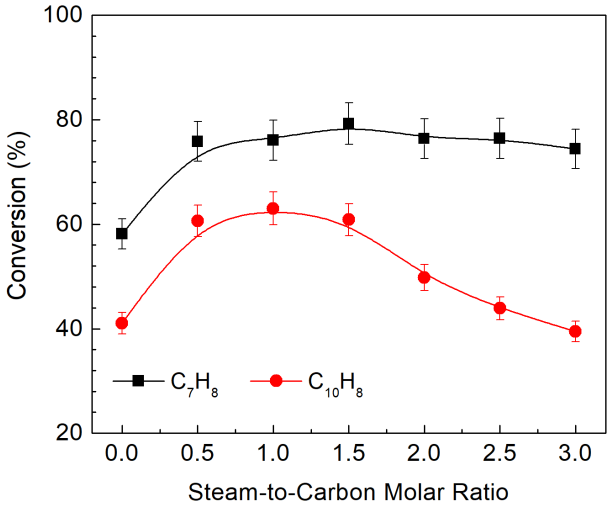

242

243 (a)

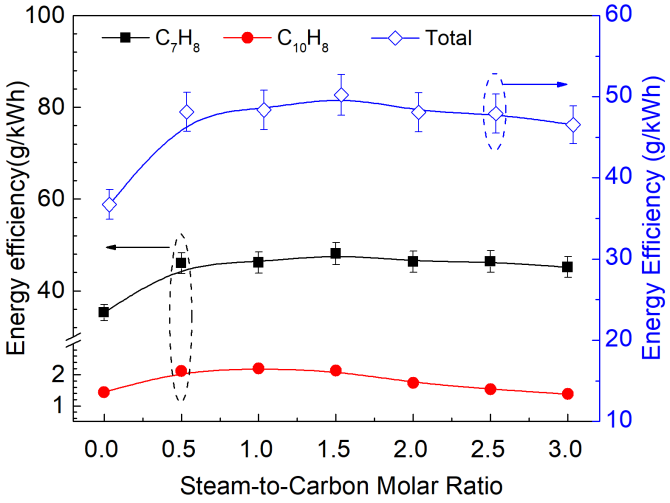

244

245 (b)

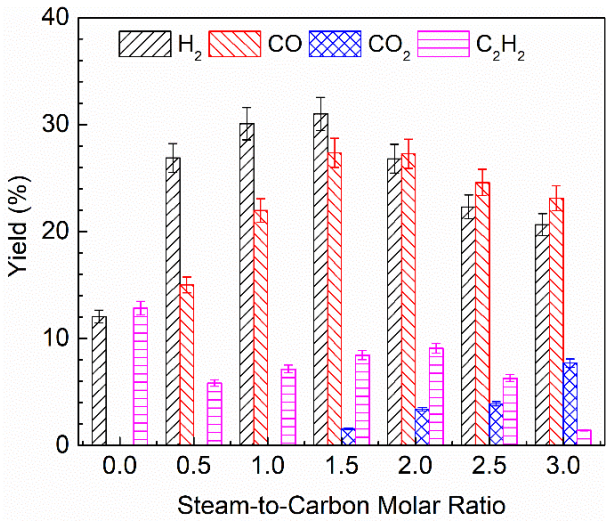

246

247 (c)

Fig. 3. Influence of steam/carbon ratio on (a) conversion of $C_{10}H_8$ and C_7H_8; (b) process efficiency; (c) yield of primary gaseous products (C_7H_8 content: 17.3 g/Nm^3; $C_{10}H_8$ content: 1.0 g/Nm^3; discharge power: 59.4 W)

However, increasing steam content in the mixed stream did not always increase the conversion of naphthalene and toluene. An optimal steam concentration can be found to reach the highest conversion of $C_{10}H_8$ or C_7H_8. Although the presence of OH radicals could provide new reaction routes for tar cracking, electrons could also be consumed by water due to its electronegative characteristic (R6) especially at a higher steam content, which in turn reduces the availability of electrons and reactive species for tar conversion.

$$H_2O + e \rightarrow H_2O^- \quad \text{(R6)}$$

The influence of H_2O on the destruction of $C_{10}H_8$ or C_7H_8 is thus dependent on the balance between these two opposite effects on the plasma reaction: i) enhanced tar conversion through additional oxidation routes due to the positive contribution of OH radicals and ii) reduced tar conversion resulted from the negative effect of electron attachment on water molecules. Such a phenomenon was also reported in our previous work where the maximum conversion of toluene (42.2%) was obtained when the ratio of steam/carbon was 2.0-3.0 in the plasma decomposition of C_7H_8 [12]. Lu et al. reported that increasing the concentration of H_2O up to 300 mg/m^3 in the feed gas stream enhanced the removal of toluene in a DC rotating GAD reactor [34]. Recently, Nunnally and co-workers found an optimal moisture content of 30% to achieve the highest removal of naphthalene and toluene in the tar decomposition in an RGA reactor [35]. The change of the process efficiency with the ratio of steam/carbon exhibited the same trend. Fig. 3(b) shows the highest energy efficiency for mixed tar conversion was about 50.2 g/kWh at the steam/carbon molar ratio of 1.5. These results indicated that the GAD can crack biomass tars with a large treatment capacity and a high energy efficiency.

Fig. 3(c) presents the yield of primary gas products in the GAD reforming under different ratios of steam/carbon. The highest yield of H_2 and CO was obtained at the optimal molar ratio of steam/carbon (1.5), beyond which the yield of H_2 and CO gradually reduced from 31.0% to 20.6% and from 27.4% to 23.1%, respectively by further enhancing S/C ratio to 3.0. CO_2 was formed only at a relatively high steam/carbon ratio (1.5-3.0), and the yield of CO_2 increased when varying the ratio of steam/carbon from 1.5 to 3.0. Recent works of plasma modeling have demonstrated that R7 is the major reaction to generate CO_2 in the plasma decomposition of naphthalene and toluene [36, 37].

$$CO + OH \rightarrow CO_2 + H \quad \text{(R7)}$$

In addition, carbon dioxide might also be formed through the water gas shift reaction [38]. Note that CO_2 is not a desirable gas product. In this study, the optimal ratio of steam/carbon should be controlled in the arrange of 1.0-1.5 to maximize the conversion of tars, the yield of CO and H_2 as well as the energy efficiency.

By contrast, the highest C_2H_2 yield (12.8%) was obtained in the GAD decomposition of mixed tar with no steam, while the presence of H_2O in the plasma reforming decreased the production of C_2H_2. Interestingly, in the presence of steam, the yield of C_2H_2 was initially enhanced with increasing the steam/carbon ratio, reaching a plateau at the steam/carbon ratio of 2.0. This value was declined when the steam/carbon ratio varied from 2.0 to 3.0. C_2H_2 is mainly formed through the cleavage of benzene rings by electrons and metastable nitrogen species (R8-R11)[39]. Adding H_2O to the plasma reaction produces oxidative species (e.g., OH radicals), which can oxidize C_2H_2 and limit the formation of C_2H_2 in this reaction. On the other hand, electrons could be attached by water (R6) due to its electronegative characteristic especially at a higher S/C ratio, which in turn reduces the formation of electrons, and consequently generates

less oxidative species such as OH radicals. In the GAD decomposition of tars, the influence of steam/carbon ratio on the yield of C_2H_2 is thus strongly associated with these correlated effects.

$$C_{10}H_8 + e \rightarrow C_8H_6 + C_2H_2 + e \quad \text{(R8)}$$

$$C_7H_8 + e \rightarrow C_5H_6 + C_2H_2 + e \quad \text{(R9)}$$

$$C_{10}H_8 + N_2^* \rightarrow C_8H_6 + C_2H_2 + N_2 \quad \text{(R10)}$$

$$C_7H_8 + N_2^* \rightarrow C_5H_6 + C_2H_2 + N_2 \quad \text{(R11)}$$

In the plasma processing of mixed naphthalene and toluene without steam, carbon deposition can be found in the GAD reactor (e.g., on the electrode surfaces and the inner wall of the reactor chamber. In our previous works, we found that the deposited carbon mainly existed in the form of spherical carbon nanoparticles in the plasma reforming of hydrocarbons (e.g., CH_4 and tars) using a similar GAD reactor [30, 40]. Note that the presence of steam in the plasma reforming process reduced the carbon deposition. As a result, the carbon balance was increased with the increase of the S/C ratio and reached a maximum of 64.0%.

3.2 Influence of naphthalene concentration

The naphthalene concentration in the tar mixture also affected the plasma destruction of naphthalene with toluene (Fig. 4). Increasing the initial naphthalene concentration from 0.49-1.83 g/Nm^3 significantly decreased the conversion of naphthalene from 72.9% to 48.9%. Interestingly, the conversion of toluene gradually decreased when increasing the naphthalene concentration. This finding can be attributed to the availability of active species and electrons in the plasma reforming process when changing the content of naphthalene and toluene in the mixed tar. Fig. 4 (b) reveals the energy efficiency of naphthalene removal increased almost linearly by a factor of 3 when increasing the initial naphthalene concentration up to 1.83 g/Nm^3. Increasing the initial concentration of naphthalene decreased the conversion of naphthalene but

increased the converted amount of naphthalene in this reforming process. The latter effect was more dominant compared to the former effect in this process, resulting in the enhanced energy efficiency for naphthalene conversion. The energy efficiency of toluene conversion dropped from 52.2 to 41.1 g/kWh due to the decrease of toluene conversion at a constant plasma power but a decreasing toluene feed. The highest energy efficiency for total tar conversion was about 53.6 g/kWh when the initial naphthalene concentration was 0.49 g/Nm^3.

The H_2 yield was almost unchanged when varying the concentration of naphthalene from 0.49 to 0.95 g/Nm^3, and then gradually decreased to 27.8% at a naphthalene content of 1.83 g/Nm^3, which could be related to the changes of the conversion of tars as a function of the naphthalene content. Similarly, CO was initially increased slightly with rising the concentration of naphthalene, reaching a peak value of 29.3% at a naphthalene content of 1.40 g/Nm^3, beyond which it decreased when further increasing naphthalene feed which can be ascribed to the reduced conversion of both tar model compounds. C_2H_2 was identified as a major hydrocarbon with the highest yield of 10.2% achieved at a naphthalene content of 1.40 g/Nm^3, while only trace amounts of other hydrocarbons (C_2H_4, C_2H_6, and C_3H_8) were formed with a total yield lower than 1%. The carbon balance increased with the concentration of naphthalene initially, reached a maximum of 60.4% at a naphthalene content of 1.40 g/Nm3 and then dropped to 52.4%, showing the same evolution as the yield of CO and C_2H_2.

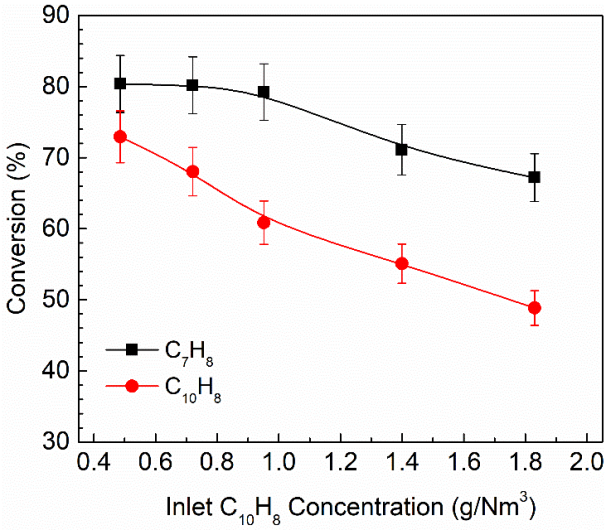

341

342 (a)

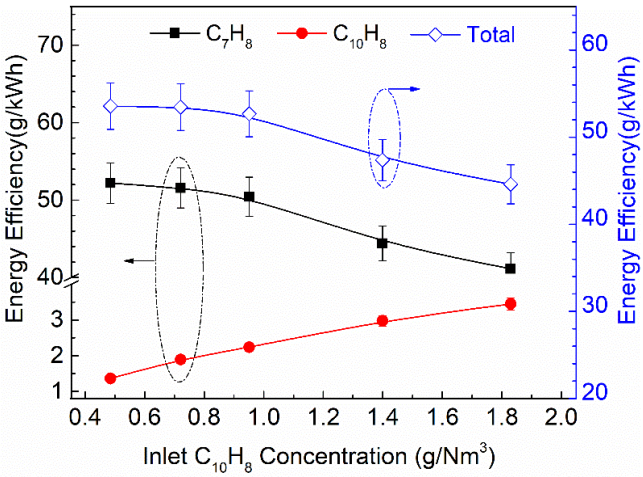

343

344 (b)

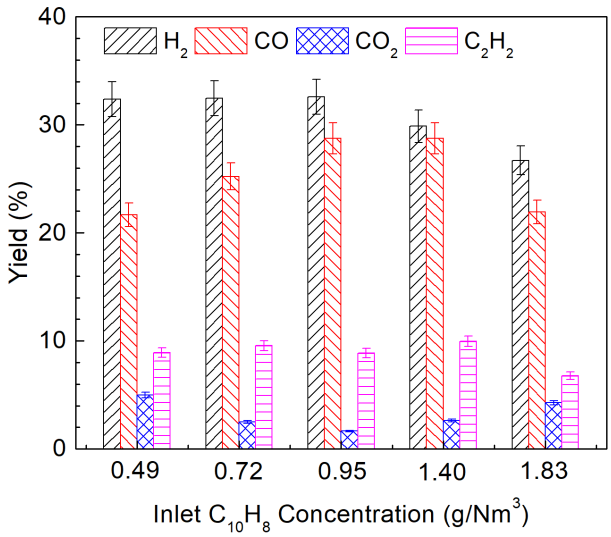

345

346 (c)

Fig. 4. Influence of initial naphthalene content on (a) conversion of $C_{10}H_8$ and C_7H_8; (b) process efficiency; (c) yield of primary gaseous products (Discharge power: 57.2 W; total tar content: 17.3 g/Nm^3; the molar ratio of S/C: 1.5)

3.3 Influence of plasma power

The influence of plasma power on the decomposition of mixed naphthalene and toluene was examined when keeping other operating parameters constant (Fig. 5). Varying the discharge power from 54.2 to 73.0 W increased the conversion of toluene by 23%, but enhanced the conversion of naphthalene conversion by 1.6 times. The yield of major gas products including H_2, CO and C_2H_2 exhibited the same evolution as the removal of tars when changing the discharge power (Fig. 5(c)). As a result, the carbon balance increased from 44.9% to 72.1% when increasing the power from 54.2 to 73.0 W. Increasing discharge power generates more high energy electrons and active species, which play a critical role in the initiation of reactions for cracking naphthalene, toluene, and their intermediates, resulted in the enhanced conversions of both tar model compounds. This effect is more prominent in the conversion of naphthalene due to its low feed concentration. In addition, the energy efficiency for the total tar conversion reached a maximum of 50.8 g/kWh (48.6 g/kWh for toluene and 2.2 g/kWh for naphthalene) in the plasma reforming process respectively, at a plasma power of 59.4 W, and then slightly declined when the plasma power was further increased even a higher conversion was obtained at a higher plasma power. Note the gas product CO_2 was not detected at a power of 54.2 W but was formed at higher discharge power (59.4-73.0 W) which could be ascribed to the promoted oxidation of tars as more oxidative species could be generated when increasing plasma power. The change of CO_2 yield with the discharge power also followed the same tendency as the conversion of naphthalene.

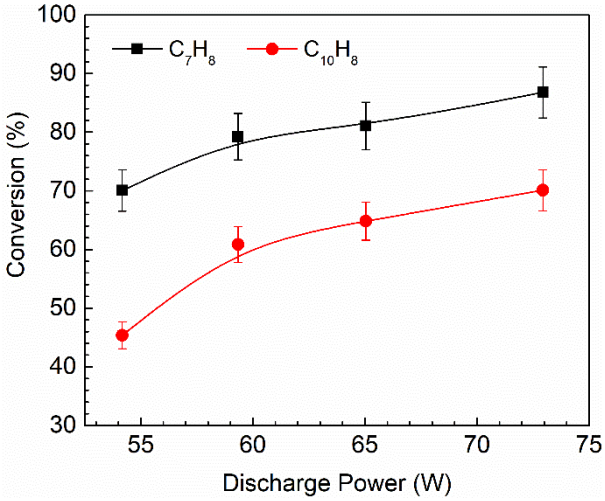
C7H8
C10H8
Conversion (%)
Discharge Power (W)

(a)

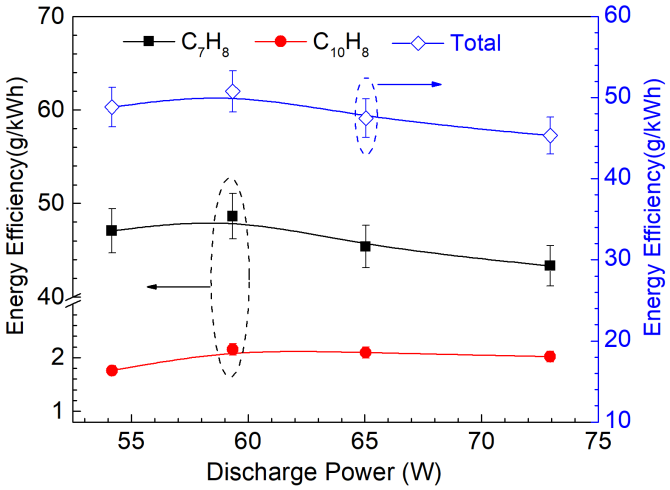
C7H8
C10H8
Total
Energy Efficiency(g/kWh)
Energy Efficiency(g/kWh)
Discharge Power (W)

(b)

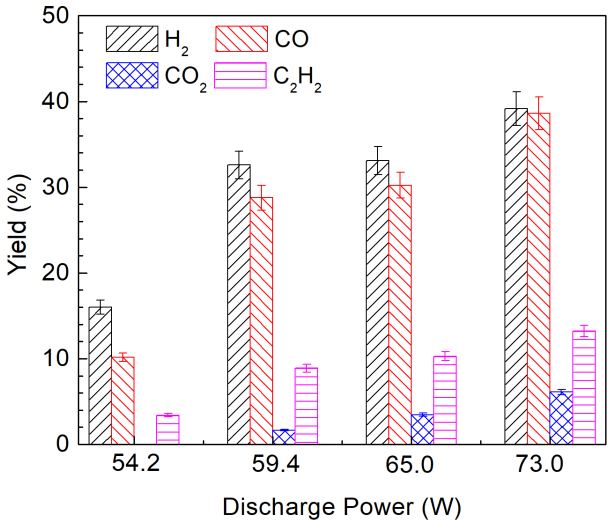
H2
CO
CO2
C2H2
Yield (%)
Discharge Power (W)

(c)

Fig. 5. Influence of plasma power on (a) conversion of $C_{10}H_8$ and C_7H_8; (b) process efficiency; (c) yield of primary gaseous products (C_7H_8 content: 16.5 g/Nm^3; $C_{10}H_8$ content: 0.95 g/Nm^3; S/C molar ratio: 1.5)

3.4 Reaction mechanisms

To better understand the production of chemically reactive species and their contributions to the plasma decomposition of naphthalene and toluene, OES was performed to record the emission of the GAD with/without steam. The effect of steam on the spectra of the GAD is shown in Fig. 6. In the absence of steam, the spectrum of the N_2/tar GAD was dominated by CN ($B^2\sum \rightarrow X^2\sum$) violet system between 350 and 420 nm. In addition, C_2 swan bands ($d^3\Pi_g \rightarrow a^3\Pi_u$) at 470-560 nm were also observed.

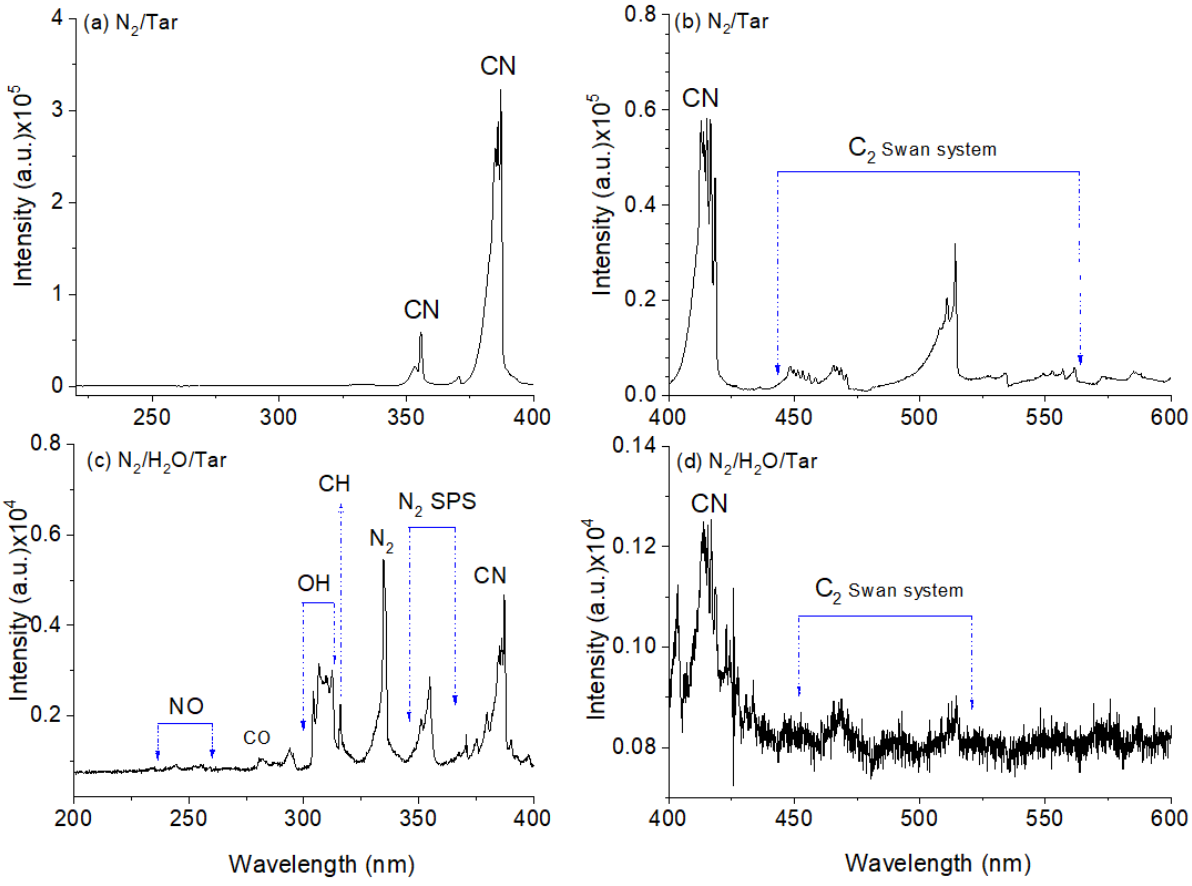

Fig. 6. Emission spectra of the GAD with/without H_2O. (C_7H_8 content: 16.5 g/m^3; $C_{10}H_8$ content: 0.95 g/m^3; discharge power: 59.4 W; grating: 600 g/mm; exposure time: 0.2 s).

Adding steam into the N_2/tar GAD showed the formation of OH radicals ($A^2\sum^+ \rightarrow X^2\prod$, 305-310 nm) in addition to CN and C_2 molecular bands. However, the presence of H_2O changed the reaction routes and significantly decreased the intensity of C_2 and CN bands. In addition, the emission of CH ($C^2\Pi^+ \rightarrow X^2\Pi$) at 314 nm, nitrogen second positive system and a weak CO band at 283 nm were also detected in the N_2/tar GAD containing steam.

The initial decomposition of toluene or naphthalene in the gliding arc can be mainly achieved through H-abstraction or cleavage of benzene ring by energetic electrons or excited nitrogen species (R12-15). Previous experimental and modeling results showed that excited nitrogen species significantly contributed to the dissociation of low concentration reactants in the plasma [31, 39, 41]. Yu and co-workers reported that the decomposition of low concentration naphthalene (~100 ppm) in a GAD system was mainly initiated by the collisions of naphthalene with excited N_2 states [41]. Trushkin et al. reported that excited N_2 species including N_2 (A^3) and N_2 (a'), contributed significantly to the initial dissociation of toluene, based on the simulation of plasma decomposition of toluene [39]. Compare to nitrogen excited species, electron impact dissociation had an insignificant role in the dissociation of $C_{10}H_8$ and C_7H_8 due to the presence of diluted reactants ($C_{10}H_8$ and C_7H_8) and small electron cross section of these hydrocarbons. Aerts and co-workers developed a plasma chemical kinetic model to gain a new insight into the reaction mechanism involving the oxidation of low concentration ethylene (10-1000 ppm) using an air DBD plasma [42]. They found that electron induced dissociation is negligible in the decomposition of C_2H_4. The fragments of toluene and

414 naphthalene can be further dissociated by excited nitrogen species or step-wised oxidized by
415 OH and O radicals to form carbon oxides, H_2O and organic by-products.

416 $$C_{10}H_8 + e \rightarrow \text{Intermediates} + e \quad \text{(R12)}$$

417 $$C_7H_8 + e \rightarrow \text{Intermediates} + e \quad \text{(R13)}$$

418 $$C_{10}H_8 + N_2^* \rightarrow \text{Intermediates} + N_2 \quad \text{(R14)}$$

419 $$C_7H_8 + N_2^* \rightarrow \text{Intermediates} + N_2 \quad \text{(R15)}$$

420

421 Plasma reforming of mixed naphthalene and toluene is a very complex process as numerous
422 chemical reactions take place simultaneously. Fig. 7 shows the GC/MS analysis of the
423 condensed liquid products collected from the GAD steam reforming of mixed naphthalene and
424 toluene. The peak area percentage of each liquid product is given in Table 1. Benzene,
425 ethylbenzene, styrene and indene were major by-products formed in the GAD reforming of
426 mixed tar compounds. Trace amounts of o-xylene, phenylethyne and acenaphthylene, and
427 oxygen-containing by-products (glyoxalic acid, oxalic acid, and diphenyl ether) were also
428 identified in this process. The generation of oxygen-containing by-products is attributed to the
429 contribution of oxidative species (e.g., OH and O radicals) in the NTP process due to the
430 presence of steam. In addition, the formation of aliphatic compounds (i.e., dibutyl phthalate
431 and 1-butene,3-methyl) suggested that ring-opening reactions took place in the decomposition
432 of $C_{10}H_8$ and C_7H_8. The polymerization reactions also can be evidenced by the presence of
433 diphenyl ether and bibenzyl. Fig. 8 shows the proposed reaction pathways through a
434 comprehensive analysis of gas and by-products combined with optical emission spectroscopic
435 diagnostics.

436

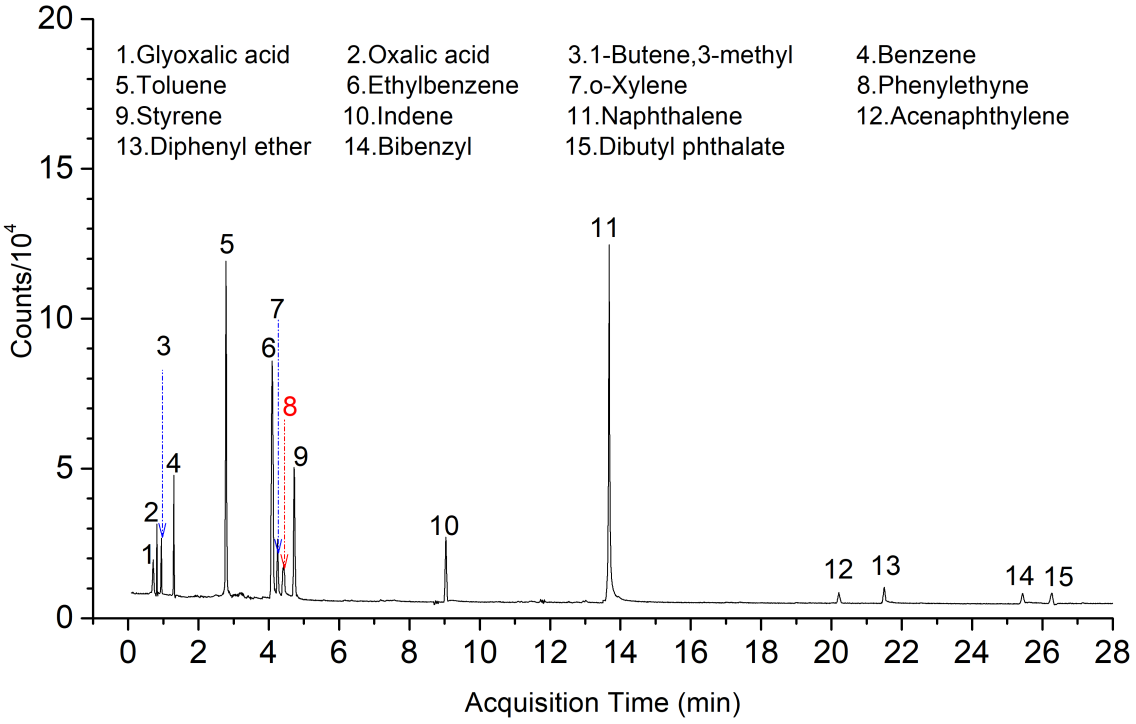

Fig. 7. GC/MS analysis of liquid samples collected from plasma steam reforming of mixed naphthalene and toluene (C_7H_8 content: 17.3 g/Nm^3; $C_{10}H_8$ content: 1.0 g/Nm^3; discharge power: 59.4 W).

Table 1 Liquid samples identified by GC/MS (C_7H_8 content: 17.3 g/Nm^3; $C_{10}H_8$ content: 1.0 g/Nm^3; discharge power: 59.4 W).

No	Compounds	Area percentage (%)	No	Compounds	Area percentage (%)
1	Glyoxalic acid	2.06	9	Styrene	8.47
2	Oxalic acid	1.38	10	Indene	4.95
3	1-Butene,3-methyl	2.06	11	Naphthalene	26.41
4	Benzene	3.44	12	Acenaphthylene	1.08
5	Toluene	18.73	13	Diphenyl ether	1.29
6	Ethylbenzene	21.80	14	Bibenzyl	1.10
7	o-Xylene	2.67	15	Dibutyl phthalate	1.48
8	Phenylethyne	3.04	Total percentage (%)		100

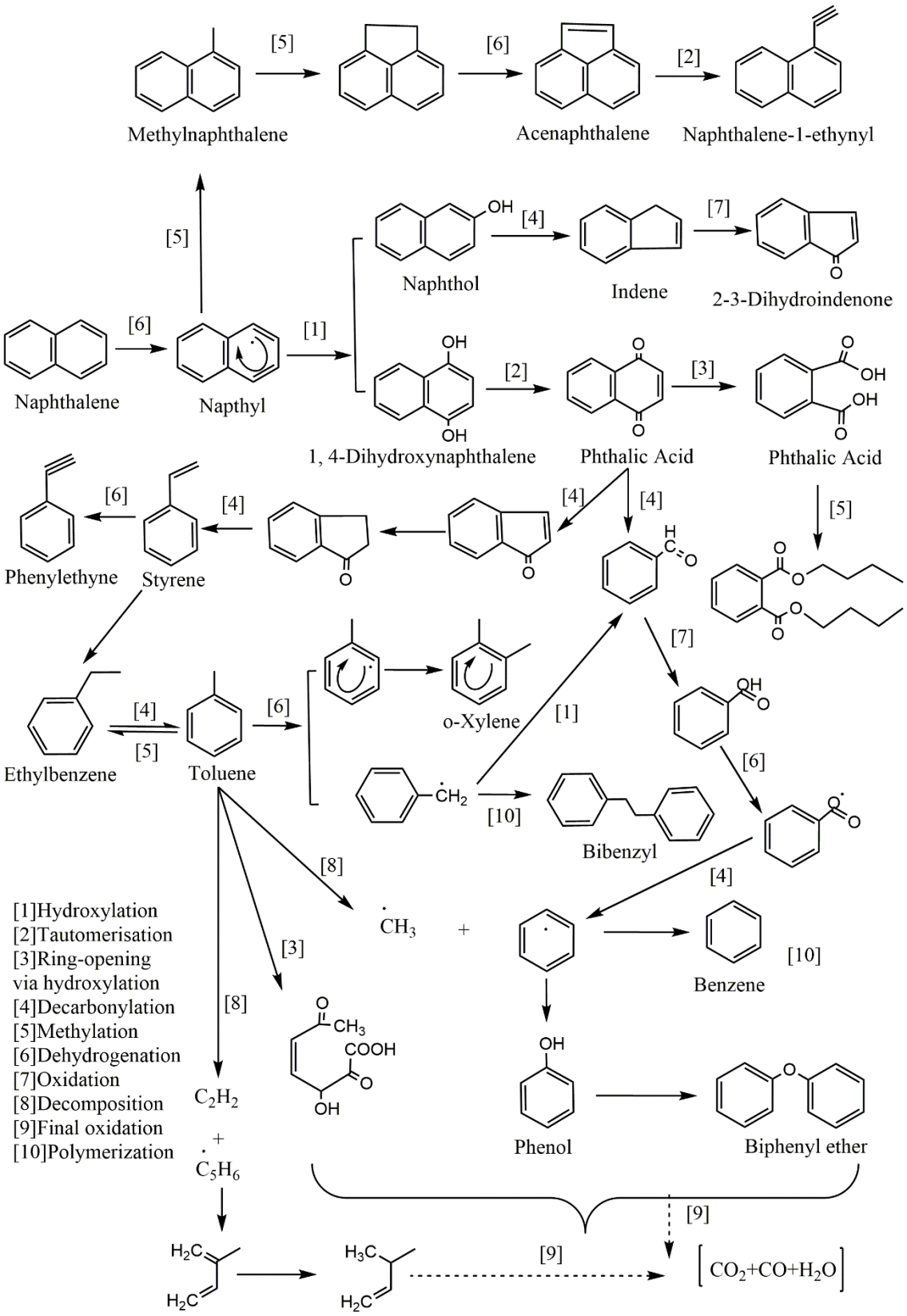

Fig. 8 Proposed reaction mechanism of plasma reforming of $C_{10}H_8$ and C_7H_8

Toluene molecules can be oxidized to produce benzaldehydes and then benzoic acid due to the presence of oxidative species, followed by the production of phenyl radicals and CO_2 via the photo-Kolbe reaction. The reaction of phenyl radicals with H forms benzene [43]. In addition, the oxidation of an aromatic ring of toluene could form an intricate hydroxyl-cyclohexadienyl type peroxy radical, which was shown in previous experimental and modeling studies [44]. Unstable reactive intermediates could actively interact with O radicals, resulted in the formation of peroxide bridge radicals for the epoxide and carbonyl reaction routes, as showed in Fig 9. The carbonyl reaction breaks a toluene ring via step-wised oxidation by O and OH radicals to generate stable oxygen-enriched compounds [12]. Meanwhile, the ring-cleavage aromatic compounds might be further fragmented and consequently mineralized into syngas and H_2O [12, 45].

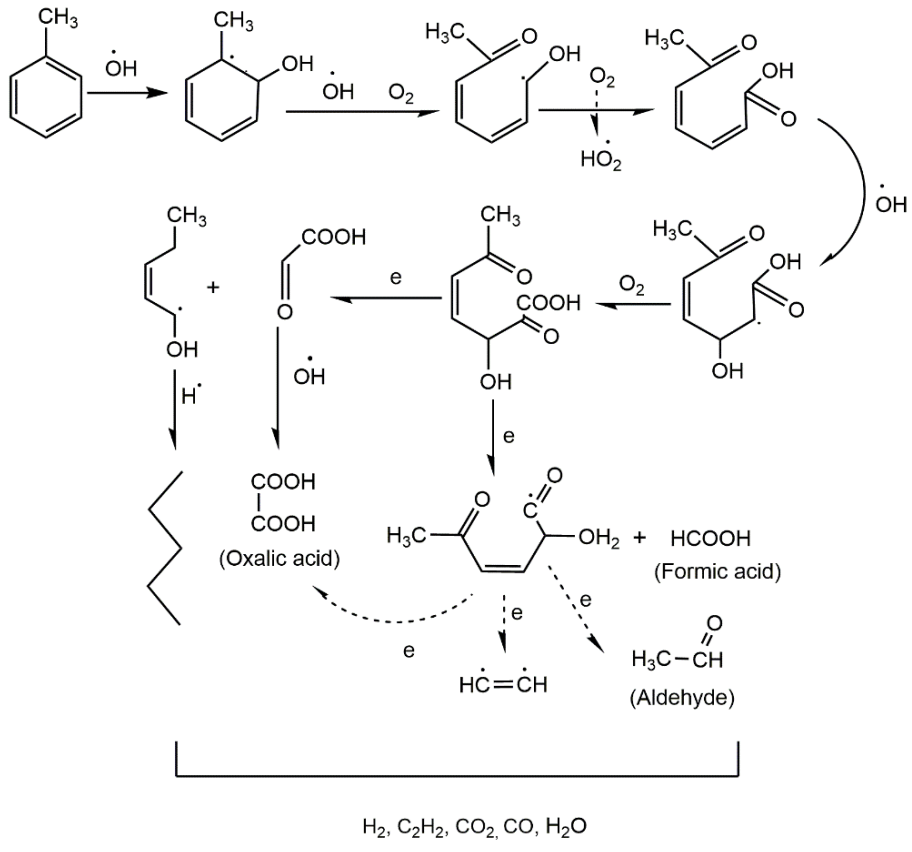

Fig. 9 Main reaction routes in the oxidation of the toluene

Similarly, the oxidation of 1,4-naphthoquinone formed from the hydroxylation of naphthalene leads to break an aromatic ring with the formation of benzaldehyde and phthalic acid, while phthalic acid can be further reacted with C_2 or C_3 entities to generate stable dibutyl phthalate. The main pathways for the generation of benzaldehyde and phthalic acid are illustrated in Fig. 10. Previous studies showed that the intermediates of naphthalene oxidation include phthalic acid, benzoin acid, benzaldehyde, phenol and other substituted aromatic alcohols[46]. Diphenyl ether and bibenzyl were detected in the condensed liquid samples in the GAD reduction of mixed $C_{10}H_8$ and C_7H_8 with steam, which could be formed by the dimerization of phenol and toluene, respectively[43]. These intermediates formed in the plasma decomposition process can be further oxidized by OH and O radicals into permanent molecules such as CO, CO_2, and H_2O.

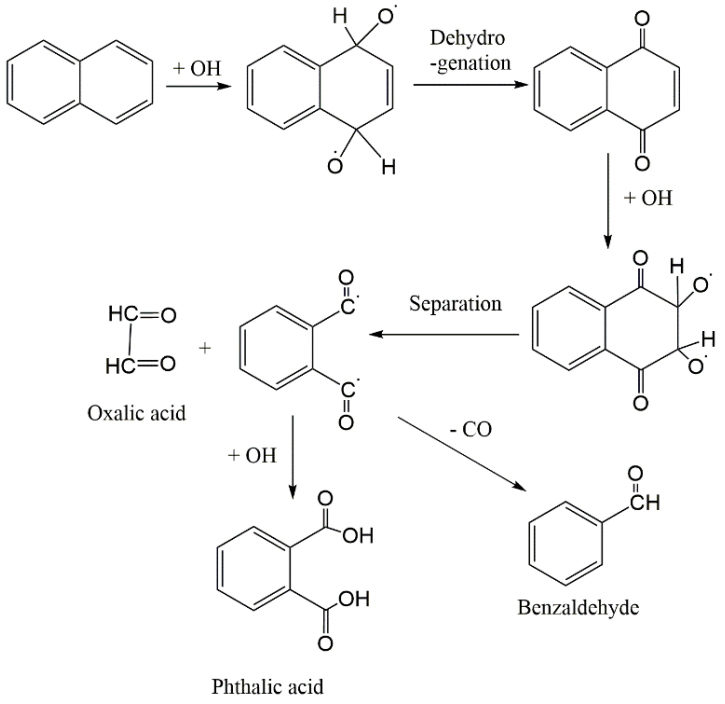

Fig. 10 Main reactions for the formation of benzaldehyde and phthalic acid

3.5 Comparison of tar reforming using different plasma processes

To assess the effectiveness of the plasma tar reforming process, Table 2 summarizes the conversion of three typical tar components (naphthalene, benzene, and toluene) and related energy efficiency for tar decomposition using different NTP technologies. Clearly, the overall energy efficiency (53.6 g/kWh) of tar conversion achieved in this study was very promising and was much higher than the result reported in previous works. We also found that GAD systems showed significantly higher energy efficiency than that using either corona or DBD, which is partly ascribed to the generation of larger electron number density in the GAD, making GAD very suitable for gas conversion or decomposition, especially for the conversion of large carbon molecules. Similar findings were also found in the processing of C1 molecules (e.g., CO_2 and CH_4) using different NTP systems, of which GAD process showed much higher efficiency for CO_2 conversion and CH_4 activation in comparison with other NTP systems such as corona and DBD [40]. Previous studies found the electron number density of a similar nitrogen GAD was ~ 10^{23} m^{-3}, which was comparable to the electron density of high temperature thermal plasma arcs and was several orders of magnitude larger than that of corona discharges (10^{15} - 10^{19} m^{-3}) and DBD plasmas (10^{16} - 10^{19} m^{-3}) [40]. Although 99% conversion of toluene was achieved using a microwave discharge reactor, the process efficiency was only 4.5 g/kWh due to the presence of low content of toluene (4.2 g/Nm^3) in the feed at a relatively higher energy input. The value of energy efficiency obtained in the microwave plasma process was quite low compared to that using other NTP systems (Table 1). Optimization of the plasma process to balance and maximize the process efficiency and the conversion is important for the development of this emerging technology for syngas cleaning. The performance of plasma bio-syngas cleaning processes for tar removal can be further improved through the development of new reactor configurations, the assessment of different power sources and the optimization of processing parameters [32, 47]. For example, Nair et al. reported that more energy was required to completely decompose tars using a

DC/AC corona process compared to that using a pulsed plasma [48]. Martens et al. also found that using a rectangular pulse can significantly reduce the energy consumption of a plasma chemical reaction by four times compared to that using a sinusoidal voltage [49]. The generation of undesirable and unwanted by-products in this plasma tar reforming process remains a challenge. The coupling of a plasma system with appropriate catalysts might offer a promising solution to enhance the process performance and to limit the production of undesirable by-products.

Table 2 Process performance for the removal of typical tar components using different NTP technologies

Plasma	Tar	Tar concentration (g/Nm^3)	Carrier gas	SEI (kWh/m^3)	Conversion (%)	Energy Efficiency (g/kWh)	Ref
Microwave Plasma	C_7H_8	4.2	20%Ar/N_2	0.93	99.0	4.5	[50]
GAD	C_6H_6	4.3	Humid N_2	0.17	82.6	20.9	[51]
DBD	C_7H_8	51.9	Humid N_2	2.00	64.0	16.7	[52]
Corona	Real tar	0.7	Real producer gas	0.04	62.0	11.2	[53]
Rotating GAD	C_7H_8	14.0	Dry N_2	2.48	83.2	16.6	[32]
GAD	$C_{10}H_8$	14.3	Humid N_2	1.00	79.0	47	[54]
GAD	C_7H_8/$C_{10}H_8$	17.3	Humid N_2	0.27	80.2	53.6	This work

4. Conclusion

514 The plasma reforming of mixed naphthalene and toluene as common tar components was
515 examined in a GAD system. The effect of different reaction conditions (e.g., steam/carbon
516 molar ratio, initial naphthalene concentration, and discharge power) on the decomposition of
517 both reactants, the generation of gas products and the process efficiency for tar removal was
518 evaluated. In the plasma reforming reaction, an optimum S/C between 1.0 and 1.5 was found
519 to obtain the highest decomposition of $C_{10}H_8$ and C_7H_8, which was dependent on the balance
520 of two opposite effects in the plasma reaction: positive effect from the contribution of OH
521 radicals and the negative effect of electron attachment due to H_2O. Increasing the initial
522 concentration of naphthalene in the mixed naphthalene and toluene decreased the conversion
523 of $C_{10}H_8$ and C_7H_8 and the process efficiency of toluene conversion. By contrast, the energy
524 efficiency for naphthalene conversion was enhanced due to the increased converted
525 naphthalene when increasing the naphthalene concentration. The highest yield of H_2 and CO
526 as major gas products was achieved at an initial naphthalene content of 0.95 g/Nm^3. Increasing
527 the discharge power increased both the conversion of naphthalene and toluene, the yield of
528 dominant products (H_2, CO, CO_2, and C_2H_2), while the energy efficiency of the plasma
529 reforming was increased firstly and then decreased after it reached a peak. The plausible
530 reaction mechanism of tar decomposition in the plasma was proposed by the plasma
531 spectroscopic diagnostics together with the analysis of the liquid and gas products.

532

533 **Acknowledgements**

534 The authors would like to thank for the financial support from the Royal Society Newton
535 Advanced Fellowship (Ref. NAF/R1/180230), EPSRC Impact Acceleration Account (IAA)
536 and the Foundation of State Key Laboratory of Coal Combustion at HUST (No.
537 FSKLCCB1805). We acknowledge the European Union (EU) and Horizon 2020 funding

awarded under the Marie Sklodowska-Curie Action to the EUROPAH Consortium (Grant Number 722346).

References

[1] Kong M, Yang Q, Fei J, Zheng X. Experimental study of Ni/MgO catalyst in carbon dioxide reforming of toluene, a model compound of tar from biomass gasification. Int J Hydrogen Energy 2012;37:13355-64.

[2] Warsita A, Al-attab KA, Zainal ZA. Effect of water addition in a microwave assisted thermal cracking of biomass tar models. Appl Therm Eng 2017;113:722-30.

[3] Milne TA, Evans RJ, Abatzoglou N. Biomass Gasifier "Tars": Their Nature, Formation, and Conversion. USA: National Renewable Energy Laboratory 1998.

[4] Shen Y, Yoshikawa K. Recent progresses in catalytic tar elimination during biomass gasification or pyrolysis-A review. Renew Sustain Energy Rev 2013;21:371-92.

[5] Bhave AG, Vyas DK, Patel JB. A wet packed bed scrubber-based producer gas cooling-cleaning system. Renew Energy 2008;33:1716-20.

[6] Świerczyński D, Libs S, Courson C, Kiennemann A. Steam reforming of tar from a biomass gasification process over Ni/olivine catalyst using toluene as a model compound. Appl Catal B-Environ 2007;74:211-22.

[7] Chen T, Liu H, Shi P, Chen D, Song L, He H, et al. CO_2 reforming of toluene as model compound of biomass tar on Ni/Palygorskite. Fuel 2013;107:699-705.

[8] de Castro TP, Silveira EB, Rabelo-Neto RC, Borges LEP, Noronha FB. Study of the performance of Pt/Al_2O_3 and $Pt/CeO_2/Al_2O_3$ catalysts for steam reforming of toluene, methane and mixtures. Catal Today 2018;299:251-62.

[9] Zhang Z, Liu L, Shen B, Wu C. Preparation, modification and development of Ni-based catalysts for catalytic reforming of tar produced from biomass gasification. Renew Sustain Energy Rev 2018;94:1086-109.

[10] Gao NB, Wang X, Li AM, Wu CF, Yin ZF. Hydrogen production from catalytic steam reforming of benzene as tar model compound of biomass gasification. Fuel Process Technol 2016;148:380-7.

[11] Artetxe M, Alvarez J, Nahil MA, Olazar M, Williams PT. Steam reforming of different biomass tar model compounds over Ni/Al_2O_3 catalysts. Energy Convers Manag 2017;136:119-26.

[12] Liu SY, Mei DH, Wang L, Tu X. Steam reforming of toluene as biomass tar model compound in a gliding arc discharge reactor. Chem Eng J 2017;307:793-802.

[13] Sun J, Wang Q, Wang W, Wang K. Study on the synergism of steam reforming and photocatalysis for the degradation of Toluene as a tar model compound under microwave-metal discharges. Energy 2018;155:815-23.

[14] Saleem F, Zhang K, Harvey A. Temperature dependence of non-thermal plasma assisted hydrocracking of toluene to lower hydrocarbons in a dielectric barrier discharge reactor. Chem Eng J 2019;356:1062-9.

[15] Liu SY, Mei DH, Shen Z, Tu X. Nonoxidative conversion of methane in a dielectric barrier discharge reactor: prediction of reaction performance based on neural network model. J Phys Chem C 2014;118:10686-93.

[16] Mei DH, Zhu XB, Wu C, Ashford B, Williams PT, Tu X. Plasma-photocatalytic conversion of CO_2 at low temperatures: Understanding the synergistic effect of plasma-catalysis. Appl Catal B: Environ.2016;182:525-32.

[17] Gao Y, Zhang S, Sun H, Wang R, Tu X, Shao T. Highly efficient conversion of methane using microsecond and nanosecond pulsed spark discharges. Appl Energy 2018;226:534-45.

[18] Kim EH, Chun YN. VOC decomposition by a plasma-cavity combustor. Chem Eng Process 2016;104:51-7.

[19] Li L, Zhang H, Li XD, Kong XZ, Xu RY, Tay K, et al. Plasma-assisted CO_2 conversion in a gliding arc discharge: Improving performance by optimizing the reactor design. J CO2 Util 2019;29:296-303.

[20] Mei DH, Liu SY, Tu X. CO_2 reforming with methane for syngas production using a dielectric barrier discharge plasma coupled with $Ni/\gamma\text{-}Al_2O_3$ catalysts: Process optimization through response surface methodology. J CO2 Util 2017;21:314-26.

[21] Zhang H, Wang W, Li X, Han L, Yan M, Zhong Y, et al. Plasma activation of methane for hydrogen production in a N_2 rotating gliding arc warm plasma: A chemical kinetics study. Chem Eng J. 2018; 345:67-78.

[22] Wang L, Yi Y, Wu C, Guo H, Tu X. One-step reforming of CO_2 and CH_4 into high-value liquid chemicals and fuels at room temperature by plasma-driven catalysis. Angew Chem Int Ed Engl. 2017; 56:13679-83.

[23] Tu X, Gallon HJ, Twigg MV, Gorry PA, Whitehead JC. Dry reforming of methane over a Ni/Al_2O_3 catalyst in a coaxial dielectric barrier discharge reactor. J Phys D-Appl Phys. 2011; 44: 274007.

[24] Wang L, Yi Y, Guo H, Tu X. Atmospheric pressure and room temperature synthesis of methanol through plasma-catalytic hydrogenation of CO_2. ACS Catal. 2017; 8: 90-100.

[25] Liu L, Wang Q, Song J, Yang X, Sun Y. Dry reforming of model biomass pyrolysis products to syngas by dielectric barrier discharge plasma. Int J Hydrogen Energy 2018;43:10281-93.

[26] Xu B, Xie JJ, Zhan H, Yin XL, Wu CZ, Liu H. Removal of toluene as a biomass tar surrogate in a catalytic nonthermal plasma process. Energy Fuel 2018;32:10709-19.

[27] Liu L, Wang Q, Ahmad S, Yang X, Ji M, Sun Y. Steam reforming of toluene as model biomass tar to H_2-rich syngas in a DBD plasma-catalytic system. J Energy Inst 2018;91:927-39.

[28] Kong X, Zhang H, Li X, Xu R, Mubeen I, Li L, et al. Destruction of toluene, naphthalene and phenanthrene as model tar compounds in a modified rotating gliding arc discharge reactor. Catalysts 2018; 9:19.

[29] Zhang H, Zhu F, Li X, Xu R, Li L, Yan J, et al. Steam reforming of toluene and naphthalene as tar surrogate in a gliding arc discharge reactor. J Hazard Mater 2019;369:244-53.

[30] Wang Y, Yang H, Tu X. Plasma reforming of naphthalene as a tar model compound of biomass gasification. Energy Convers Manag 2019;187:593-604.

[31] Wnukowski M, Jamróz P. Microwave plasma treatment of simulated biomass syngas: Interactions between the permanent syngas compounds and their influence on the model tar compound conversion. Fuel Process Technol 2018;173:229-42.

[32] Zhu F, Li X, Zhang H, Wu A, Yan J, Ni M, et al. Destruction of toluene by rotating gliding arc discharge. Fuel 2016;176:78-85.

[33] Jamroz P, Kordylewski W, Wnukowski M. Microwave plasma application in decomposition and steam reforming of model tar compounds. Fuel Process Technol 2018;169:1-14.

[34] Lu SY, Sun XM, Li XD, Yan JH, Du CM. Decomposition of toluene in a rotating gglidarc discharge reactor. IEEE Trans Plasma Sci 2012;40:2151-6.

[35] Nunnally T, Tsangaris A, Rabinovich A, Nirenberg G, Chernets I, Fridman A. Gliding arc plasma oxidative steam reforming of a simulated syngas containing naphthalene and toluene. Int J Hydrogen Energy 2014;39:11976-89.

[36] Bityurin VA, Filimonova EA, Naidis GV, Mechanisms of conversion of heavy hydrocarbons in biogas initiated by pulsed corona discharges. In: S. Güçeri, A. Fridman, K. Gibson, C. Haas (Eds.), Plasma assisted decontamination of biological and chemical agents. NATO Science for Peace and Security Series Series A: Chemistry and Biology. Springer, Dordrecht, 2008, pp. 135-42.

[37] Bityurin VA, Filimonova EA, Naidis GV. Simulation of naphthalene conversion in biogas initiated by pulsed corona discharges. IEEE Trans Plasma Sci 2009;37:911-9.

[38] Abdelaziz AA, Seto T, Abdel-Salam M, Otani Y. Influence of N_2/O_2 mixtures on decomposition of naphthalene in surface dielectric barrier discharge based reactor. Plasma Chem Plasma Process 2014;34:1371-85.

[39] Trushkin AN, Grushin ME, Kochetov IV, Trushkin NI, Akishev YS. Decomposition of toluene in a steady-state atmospheric-pressure glow discharge. Plasma Phys Rep 2013;39:167-82.

[40] Tu X, Whitehead JC. Plasma dry reforming of methane in an atmospheric pressure AC gliding arc discharge: Co-generation of syngas and carbon nanomaterials. Int J Hydrogen Energy. 2014;39:9658-69.

[41] Yu L, Li X, Tu X, Wang Y, Lu S, Yan J. Decomposition of naphthalene by dc gliding arc gas discharge. J Phys Chem A 2010;114:360-8.

[42] Aerts R, Tu X, De Bie C, Whitehead JC, Bogaerts A. An investigation into the dominant reactions for ethylene destruction in non-thermal atmospheric plasmas. Plasma Process Polym 2012;9:994-1000.

[43] Sun J, Wang Q, Wang W, Wang K. Plasma catalytic steam reforming of a model tar compound by microwave-metal discharges. Fuel 2018;234:1278-84.

[44] Van Durme J, Dewulf J, Sysmans W, Leys C, Van Langenhove H. Abatement and degradation pathways of toluene in indoor air by positive corona discharge. Chemosphere 2007;68:1821-9.

[45] Liu SY, Mei DH, Nahil MA, Gadkari S, Gu S, Williams PT, Tu X. Hybrid plasma-catalytic steam reforming of toluene as a biomass tar model compound over Ni/Al_2O_3 catalysts. Fuel Process Technol 2017;166:269-75.

[46] Gao X, Shen X, Wu Z, Luo Z, Ni M, Cen K, The mechanism of naphthalene decomposition in corona radical shower system by DC discharge. In: K. Yan (Eds.) Electrostatic Precipitation. Springer, Berlin, Heidelberg, 2009, pp. 713-717.

667 [47] Abdelaziz AA, Seto T, Abdel-Salam M, Ishijima T, Otani Y. Influence of applied voltage
668 waveforms on the performance of surface dielectric barrier discharge reactor for
669 decomposition of naphthalene. J Phys D: Appl Phys 2015;48:195201.
670 [48] Nair SA, Yan K, Pemen AJM, van Heesch EJM, Ptasinski KJ, Drinkenburg AAH. Tar
671 removal from biomass derived fuel gas by pulsed corona discharges: Chemical Kinetic
672 Study II. Ind Eng Chem Res 2005;44:1734-41.
673 [49] Martens T, Bogaerts A, van Dijk J. Pulse shape influence on the atmospheric barrier
674 discharge. Appl Phys Lett 2010;96:131503.
675 [50] Eliott RM, Nogueira MFM, Silva Sobrinho AS, Couto BAP, Maciel HS, Lacava PT. Tar
676 reforming under a microwave plasma torch. Energy Fuel 2013;27:1174-81.
677 [51] Chun YN, Kim SC, Yoshikawa K. Decomposition of benzene as a surrogate tar in a
678 gliding Arc plasma. Environ Progress Sustain Energy 2013;32:837-45.
679 [52] Wu Z, Wang J, Han J, Yao S, Xu S, Martin P. Naphthalene decomposition by dielectric
680 barrier discharges at atmospheric pressure. IEEE Trans Plasma Sci 2017;45:154-61.
681 [53] van Heesch BEJM, Pemen GAJM, Yan KP, van Paasen SVB, Ptasinski KJ, Huijbrechts
682 PAHJ. Pulsed corona tar cracker. IEEE Trans Plasma Sci 2000;28:1571-5.
683 [54] Yang YC, Chun YN. Naphthalene destruction performance from tar model compound
684 using a gliding arc plasma reformer. Korean J Chem Eng 2011;28:539-43.
685
686